

Dual Controlled Cross - Shaped Broadband Terahertz Absorber Based On Vanadium Oxide - Liquid Crystal Metamaterial

Renxia Ning (✉ nrxiner@163.com)

Huangshan University <https://orcid.org/0000-0002-1229-7476>

Fei Wang

Huangshan University

Wang Huang

Huangshan University

Research Article

Keywords: Dual controlled, broadband absorber, vanadium oxide, liquid crystal metamaterial

Posted Date: July 27th, 2021

DOI: <https://doi.org/10.21203/rs.3.rs-735595/v1>

License:  This work is licensed under a Creative Commons Attribution 4.0 International License.

[Read Full License](#)

Abstract

A low terahertz broadband tunable absorber was proposed, which was mainly composed of vanadium oxide (VO_2) film and nematic liquid crystal layer. The simulation results show that the absorption can reach more than 90% in the range of 0.458 THz-1.1492 THz. With the vanadium oxide transitioned into metal state, the tuning absorber was realized. Since the dielectric constant of the nematic liquid crystal can be adjusted by bias voltage, without changing the intensity of absorption, but a shift in the bandwidth was observed. In addition, the structure designed in this paper was insensitive to incident light polarization and still remained high absorption at 60° . This tunable broadband metamaterial absorber can be used for attenuator and energy harvesting.

Introduction

Metamaterial absorbers have always attracted the tremendous attention owing to their significant roles in various practical applications such as sensing [1, 2], solar energy harvesting [3], thermal emission [4] and stealth technology [5, 6]. Currently, the research on narrow-band and multi-band absorbers had been relatively mature, and some of the demonstrated structures can achieve nearly 100% perfect absorption at a specific frequency [7–9]. In practical application, the broadband metamaterial absorber has a wider frequency response range fitting more frequency requirements. Two common methods are developed, localized broadband absorption is achieved through combining multiple sublattice structures of different sizes in a unit cell. For example, Cheng *et al.* realized a study in which they achieved a broadband emitter composed of a multi-sized disk array [10]. Guo *et al.* designed wideband perfect light absorber that the gold thin-film squares are periodically patterned on top of thick gold metal substrate [11]. Furthermore, using multilayer structures can achieve the bandwidth enhancement well [12–14], but the configuration of these designs is slightly more complex, and they require some complicated fabrication procedures. Alternatively, in some specific applications, such as solar cells and stealth technology, this type of application demands a very wide absorption bandwidth. In Ref. [15], He *et al.* obtained an ultra-wideband thin film infrared absorber, the corresponding relative bandwidths of above 90% absorption were 86%. In Ref. [16], Mehmet *et al.* studied a microwave energy harvesting device with 80% efficiency between 7.8 GHz and 14 GHz. Although there are many improvements in the wideband absorbers, once the structure of metamaterial absorbers is well designed, the resonance nature and absorption rate will not change, which greatly limits its application in practice. Thus, in potential applications, a tunable absorber is more attractive for the design. In recent years, a variety of dynamically tunable absorbers have been demonstrated. Metamaterials are combined with active materials such as graphene, semiconductors, liquid crystals and vanadium dioxide (VO_2) [17–20]. The methods of modulation can be listed as thermal control [21], photoexcitation [22], external voltage [23]. Among these materials, as a phase change material, the electrical conductivity can be increased by orders of magnitude [24]. Nematic liquid crystals have agile dielectric constants and relatively low dielectric losses over a wide frequency range [25].

In this study, we have proposed a broadband terahertz metamaterial absorber with dual tunable capability. The different geometrical dimensions VO_2 films tiled on the top and middle parts were

composed of nematic liquid crystal (LC) and dielectric layer. Based on the insulator-metal phase change of VO₂ and the orientation of the liquid crystal molecules can be controlled by an external bias voltage[26–28], the operation frequency was chosen from 0.458 THz to 1.1492 THz the shift resonant frequency could be observed.

Materials And Methods

We proposed a low terahertz broadband metamaterial absorber, schematic diagram is presented in Fig. 1, as shown in Fig. 1(a), the absorber has five layers, the first layer of VO₂ is made up of four proportional cross shapes and in the insulator phase the permittivity of VO₂ was $\varepsilon = 9$ [29], each resonator is located in the center of the corresponding portion. The original proportional starting from the first cross shape on the left, the proportions are 0.9, 0.8, 0.7 in clockwise direction. The middle layer is separated by polyimide between the liquid crystal and the metal substrate with the dielectric permittivity $\varepsilon_d = 3.1$. The structure of metal base plate makes the transmission is 0. The nature of metal in terahertz (THz) range is described by the Drude model with the plasma frequency $\omega_p = 1.37 \times 10^{16} \text{ s}^{-1}$,

$$\varepsilon(\omega) = \left(\mathbf{1} - \frac{\omega_p^2}{\omega^2 + j\omega\gamma} \right) \quad (1)$$

the frequency of the scattering $\gamma = 4.08 \times 10^{13} \text{ s}^{-1}$ [30]. It's periodic in the x and in the y direction and the length being $P_x = P_y = 350 \text{ }\mu\text{m}$, $l_1 = 165 \text{ }\mu\text{m}$, $d_1 = 55 \text{ }\mu\text{m}$. The side view of the structure in Fig. 1(c) shows the thickness of this structure, respectively $h_1 = 0.08 \text{ }\mu\text{m}$, $h_2 = 1.625 \text{ }\mu\text{m}$, $h_3 = 50 \text{ }\mu\text{m}$, $h_4 = 0.2 \text{ }\mu\text{m}$.

We used the finite difference time domain (FDTD) method, where x, y is the unit cell boundary condition and in the z direction is opening. According to the electromagnetic wave propagation theory on the medium interface, the amount of reflection and transmission depends on the electromagnetic wave impedance in free space and the intrinsic impedance equivalent degree of the medium. Considering the periodic structure of subwavelength, through the reflection and transmission of electromagnetic waves, absorption can be expressed by $A(\omega) = 1 - R(\omega) - T(\omega)$, $R(\omega) = |S_{11}(\omega)|^2$, $T(\omega) = |S_{22}(\omega)|^2$ respectively. $S_{11}(\omega)$ is the reflection coefficient and $S_{22}(\omega)$ is the transmission coefficient. Due to the zero transmission from the absorber, absorption ultimately equal to $1 - R(\omega)$. On the other hand, LCs are another promising material for practical applications in the terahertz range as the permittivity can be controlled by an external bias voltage. In here, the up layer and the metal ground plane are used as two electrodes and liquid crystals 4'-n-pentyl-4-cyanobiphenyl (5CB) were filled into the middle gap[31, 32]. The LC material is composed of anisotropic molecules and initial alignment direction of 5CB without bias voltage should be parallel to the electrical field direction. Therefore, the effective refractive index of 5CB could be changed with the different angles of the LC arrangement. When the closer the orientation of LC is to the direction of the external electric field, the higher the refractive index of liquid crystal is. The magnitude of the extraordinary and ordinary refractive indices are given the following $n_e = 1.77$ and $n_o = 1.58$, which the birefringence is equal to 0.20 ± 0.02 [31].

Results And Discussion

In order to demonstrate the absorption characteristics of the proposed structure, the numerical simulation results are as follows the transverse magnetic (TM) wave and the transverse electric (TE) wave have been studied and the simulation result is presented in Fig. 2. It's clear that have the similar absorption in TE and TM mode. We can also see that achieve about 97% of the absorption between 0.458 THz and 1.1492 THz. Considering the periodic structure of sub-wavelength and then the electromagnetic wave incident from free-space to the structure, its equivalent impedance Z can be expressed as [33]:

$$Z = \sqrt{\frac{(1+S_{11}^2) - S_{21}^2}{(1-S_{11}^2) - S_{21}^2}} \quad (2)$$

With perfectly normalized impedance, the real part of Z is close to 1 and the imaginary part of the impedance is close to 0 in the range of 0.458 THz – 1.1492 THz, thus resulting in minimal reflection and very high wideband absorption. To further illustrate the absorption mechanism, the distribution of electric and magnetic fields are studied at the resonant frequencies of 0.9569 THz and 1.124 THz, which absorption values are at quite high peak. The electrical field and magnetic field direction for the top layer as shown in Fig. 2. Obviously, it can be seen that VO₂ films display the different resonant frequencies, and exist coupling of different sizes in a plane, and multiple absorption bands overlap to expand the absorption band.

We also demonstrate the absorption capability of the broadband absorber that the corresponding simulation of a cross-shaped unit structure is shown in Fig. 4. It can be seen that the absorption spectrum of more than 80% have two resonant ranges, which from 0.312 THz to 1.226 THz. By reducing the size of the top pattern, from Fig. 4(b) to (d), the bandwidth of the absorption is also reduced.

Owing to the properties of the VO₂ transition from insulating to metallic states at high temperature, the tunable absorption characteristics of a broadband absorber can be realized and we set the conductivity variable from 500 S/m to 1×10⁵ S/m. Figure 5 shows the absorption spectrum of VO₂ with different electrical conductivity under normal incidence. The results indicate that with the electrical conductivity of cruciform patches 2 and 4 changes, the corresponding absorption spectrum changes accordingly. It can be seen from that the position of the bandwidth is almost constant and the intensity of the absorption spectrum changes significantly and the absorption is above 97% in the low THz frequency range. Specially, with the conductivity decreases, the absorption decreases gradually at 0.95 THz. Since the imaginary parts of VO₂ mainly affects the loss. Meanwhile, VO₂ is in conductor state, broadband tuning can also be achieved by adjusting the electric field. We give the effective dielectric constant of aligned nematic LC and the arrangement angle of it [34].

$$n_{\text{eff}} = \frac{n_e n_o}{\sqrt{n_e^2 \sin^2 \theta + n_o^2 \cos^2 \theta}} \quad (3)$$

When the orientation of the LC molecules is $\theta = 0^\circ$, the direction of the electric field is perpendicular to the LC molecules. As liquid crystals are anisotropic medium and the electric field becomes higher, its molecules direction tend to be oriented in the z direction. Through calculating the direction of the LC under $0^\circ, 30^\circ, 45^\circ, 60^\circ, 90^\circ$ corresponding to the $n_{\text{eff}} = 1.58, 1.62, 1.67, 1.72, 1.77$. Figure 6 shows that the absorption spectrum of tunable bandwidth is achieved as bias voltage is applied to the LC cell.

In Fig. 6, it was shown that broadband absorption as the LC molecule is reorientated from 0° to 90° , which can be attributed to the high absorptivity and adjust within a relatively small range. To validate the effect of the thickness of the VO_2 on absorption. It is obvious from the Fig. 7 that the absorption of the broadband absorber gradually decreases with the thickness of the VO_2 increases. The absorption reaches an optimum at $h_1 = 0.08 \mu\text{m}$. We also provide additional performance validation of the proposed absorber under different polarization angles in TM mode, incident TE waves. It can be seen from Fig. 8 that the absorption level is nearly unchanged with the increasing polarized angle, while the resonant frequency range is changed. Thus, we providing a characteristic of broadband absorber with flexible tunability, it maintains about 95% absorption above from 0.6 THz to 1.1 THz over relatively wide angles.

Conclusions

In this paper, we proposed a broadband metamaterial absorber combining two active materials, vanadium oxide and nematic liquid crystal. The simulation results show that the resonant region of the broadband absorber over 90% in which the relative bandwidth reaches 57.6%. The electric field distribution of the metamaterial absorber in the absorption wave of 0.9569 THz and 1.124 THz and the equivalent impedance of the structure response, a cross-shaped unit structure is given, and then the simulation results show that the analogous high bandwidth absorption. It is also verified that the absorber has the allied absorption for TM and TE waves, besides the absorbance is maintained at 80% when the incident angle increases to 60° in the TM mode. Additionally, the metamaterial absorber achieves tunability at lower terahertz frequencies which compared to previous metamaterial absorbers that can just achieve fixed bandwidth absorption. The vanadium oxide can be transited from an insulator to a metal at different operating temperatures, and the absorbance and bandwidth are relatively enhanced as the temperature increases. Based on the dielectric constant of nematic liquid crystal is affected by the rotation of liquid crystal molecules, thus by adjusting the bias voltage which achieve another tuning performance. Benefit from these advantages, the properties of the device provided a way for energy harvesting, imaging and other fields.

Declarations

Acknowledgment

This research was funded by Key Laboratory of Radar Imaging and Microwave Photonics (Nanjing University of Aeronautics and Astronautics), Ministry of Education (NO.NJ20210006), Natural Science

References

1. Horestani, A.K., Naqui, J., Shaterian, Z., Abbott, D., Fumeaux, C., Martín, F.: Two-dimensional alignment and displacement sensor based on movable broadside-coupled split ring resonators. *Sensors and Actuators A: Physical* **210**, 18–24 (2014)
2. Kabashin, A.V., Evans, P., Pastkovsky, S., Hendren, W., Wurtz, G.A., Atkinson, R., Pollard, R., Podolskiy, V.A., Zayats, A.V.: Plasmonic nanorod metamaterials for biosensing, *Nat Mater*, 8, 867–871(2009)
3. Wang, H., Wang, L.: Perfect selective metamaterial solar absorbers. *Opt. Express* **21**(Suppl 6), A1078–A1093 (2013)
4. Liu, X., Tyler, T., Starr, T., Starr, A.F., Jokerst, N.M., Padilla, W.J.: Taming the blackbody with infrared metamaterials as selective thermal emitters. *Phys. Rev. Lett.* **107**, 045901 (2011)
5. Kim, J., Han, K., Hahn, J.W.: Selective dual-band metamaterial perfect absorber for infrared stealth technology. *Sci Rep* **7**, 6740 (2017)
6. Ni, X., Wong, Z.J., Mrejen, M., Wang, Y., Zhang, X.: An ultrathin invisibility skin cloak for visible light. *Science* **349**, 1310–1314 (2015)
7. Liu, N., Mesch, M., Weiss, T., Hentschel, M., Giessen, H.: Infrared perfect absorber and its application as plasmonic sensor. *Nano Lett.* **10**, 2342–2348 (2010)
8. Yao, G., Ling, F., Yue, J., Luo, C., Ji, J., Yao, J.: Dual-band tunable perfect metamaterial absorber in the THz range. *Opt. Express* **24**, 1518–1527 (2016)
9. Zhang, M., Fang, J., Zhang, F., Chen, J., Yu, H.: Ultra-narrow band perfect absorbers based on Fano resonance in MIM metamaterials. *Opt. Commun.* **405**, 216–221 (2017)
10. Cheng, C.W., Abbas, M.N., Chiu, C.W., Lai, K.T., Shih, M.H., Chang, Y.C.: Wide-angle polarization independent infrared broadband absorbers based on metallic multi-sized disk arrays. *Opt. Express* **20**, 10376–10381 (2012)
11. Hendrickson, J., Guo, J., Zhang, B., Buchwald, W., Soref, R.: Wideband perfect light absorber at midwave infrared using multiplexed metal structures. *Opt Lett* **37**, 371–373 (2012)
12. Sun, J., Liu, L., Dong, G., Zhou, J.: An extremely broad band metamaterial absorber based on destructive interference. *Opt. Express* **19**, 21155–21162 (2011)
13. Liu, S., Chen, H., Cui, T.J.: A broadband terahertz absorber using multi-layer stacked bars. *Appl. Phys. Lett.* **106**, 151601 (2015)
14. Deng, H., Stan, L., Czaplewski, D.A., Gao, J., Yang, X.: Broadband infrared absorbers with stacked double chromium ring resonators. *Opt. Express* **25**, 28295–28340 (2017)
15. Liu, H., Wang, Z.-H., Li, L., Fan, Y.-X., Tao, Z.-Y.: Vanadium dioxide-assisted broadband tunable terahertz metamaterial absorber. *Sci. Rep.* **9**, 5751 (2019)

16. Su, H., Wang, H., Zhao, H., Xue, T., Zhang, J.: Liquid-Crystal-Based Electrically Tuned Electromagnetically Induced Transparency Metasurface Switch. *Sci Rep* **7**, 17378 (2017)
17. Chen, F., Cheng, Y., Luo, H.: A Broadband Tunable Terahertz Metamaterial Absorber Based on Single-Layer Complementary Gammadion-Shaped Graphene. *Materials (Basel)* **13**, 860 (2020)
18. Zhang, Y., Feng, Y., Zhu, B., Zhao, J., Jiang, T.: Graphene based tunable metamaterial absorber and polarization modulation in terahertz frequency. *Opt. Express* **22**, 22743–22752 (2014)
19. Deng, G., Xia, T., Jing, S., Yang, J., Lu, H., Yin, Z.: A Tunable Metamaterial Absorber Based on Liquid Crystal Intended for F Frequency Band. *IEEE Antennas Wirel. Propag. Lett.* **16**, 2062–2065 (2017)
20. Tian, X., Li, Z.-Y.: An Optically-Triggered Switchable Mid-Infrared Perfect Absorber Based on Phase-Change Material of Vanadium Dioxide, *Plasmonics*, **13**, 1393–1402(2017)
21. Wen, Q.-Y., Zhang, H.-W., Yang, Q.-H., Xie, Y.-S., Chen, K., Liu, Y.-L.: Terahertz metamaterials with VO₂ cut-wires for thermal tunability. *Appl. Phys. Lett.* **97**, 021111 (2010)
22. Cheng, Y., Gong, R., Cheng, Z.: A photoexcited broadband switchable metamaterial absorber with polarization-insensitive and wide-angle absorption for terahertz waves. *Opt. Commun.* **361**, 41–46 (2016)
23. Jiang, W., Yan, L., Ma, H., Fan, Y., Wang, J., Feng, M., Qu, S.: Electromagnetic wave absorption and compressive behavior of a three-dimensional metamaterial absorber based on 3D printed honeycomb. *Sci Rep* **8**, 4817 (2018)
24. Song, Z., Wei, M., Wang, Z., Cai, G., Liu, Y., Zhou, Y.: Terahertz Absorber With Reconfigurable Bandwidth Based on Isotropic Vanadium Dioxide Metasurfaces. *IEEE Photonics J.* **11**, 1–7 (2019)
25. Yin, Z., Lu, Y., Xia, T., Lai, W., Yang, J., Lu, H., Deng, G.: Electrically tunable terahertz dual-band metamaterial absorber based on a liquid crystal. *RSC Advances* **8**, 4197–4203 (2018)
26. Wu, G., Jiao, X., Wang, Y., Zhao, Z., Wang, Y., Liu, J.: Ultra-wideband tunable metamaterial perfect absorber based on vanadium dioxide. *Opt. Express* **29**, 2703–2711 (2021)
27. Wang, P.-Y., Jin, T., Meng, F.-Y., Lyu, Y.-L., Erni, D., Wu, Q., Zhu, L.: Numerical investigation of nematic liquid crystals in the THz band based on EIT sensor. *Opt. Express* **26**, 12318–12329 (2018)
28. Su, Z., Yin, J., Zhao, X.: Soft and broadband infrared metamaterial absorber based on gold nanorod/liquid crystal hybrid with tunable total absorption. *Sci Rep* **5**, 16698 (2015)
29. Huang, J., Li, J., Yang, Y., Li, J., Li, J., Zhang, Y., Yao, J.: Active controllable dual broadband terahertz absorber based on hybrid metamaterials with vanadium dioxide. *Opt. Express* **28**, 7018–7027 (2020)
30. Ordal, M.A., Long, L.L., Bell, R.J., Bell, S.E., Bell, R.R., Alexander, R.W. Jr., Ward, C.A.: Optical properties of the metals Al, Co, Cu, Au, Fe, Pb, Ni, Pd, Pt, Ag, Ti, and W in the infrared and far infrared, *Appl Opt*, **22**, 1099 – 1020(1983)
31. Pan, R.-P., Hsieh, C.-F., Pan, C.-L., Chen, C.-Y.: Temperature-dependent optical constants and birefringence of nematic liquid crystal 5CB in the terahertz frequency range, *Journal of Applied Physics*, **103**, (2008)

32. Wu, Y., Ruan, X., Chen, C.H., Shin, Y.J., Lee, Y., Niu, J., Liu, J., Chen, Y., Yang, K.L., Zhang, X., Ahn, J.H., Yang, H.: Graphene/liquid crystal based terahertz phase shifters. *Opt. Express* **21**, 21395–21402 (2013)
33. Bağmancı, M., Karaaslan, M., Altıntaş, O., Karadağ, F., Tetik, E., Bakır, M.: Wideband metamaterial absorber based on CRRs with lumped elements for microwave energy harvesting. *J. Microw. Power Electromagn. Energy*. **52**, 45–59 (2017)
34. Oh, E.M., Yokoyama, H., Koeberg, M., Hendry, E., Bonn, M.: High-frequency dielectric relaxation of liquid crystals: THz time-domain spectroscopy of liquid crystal colloids. *Opt. Express* **14**, 11433–11441 (2006)

Figures

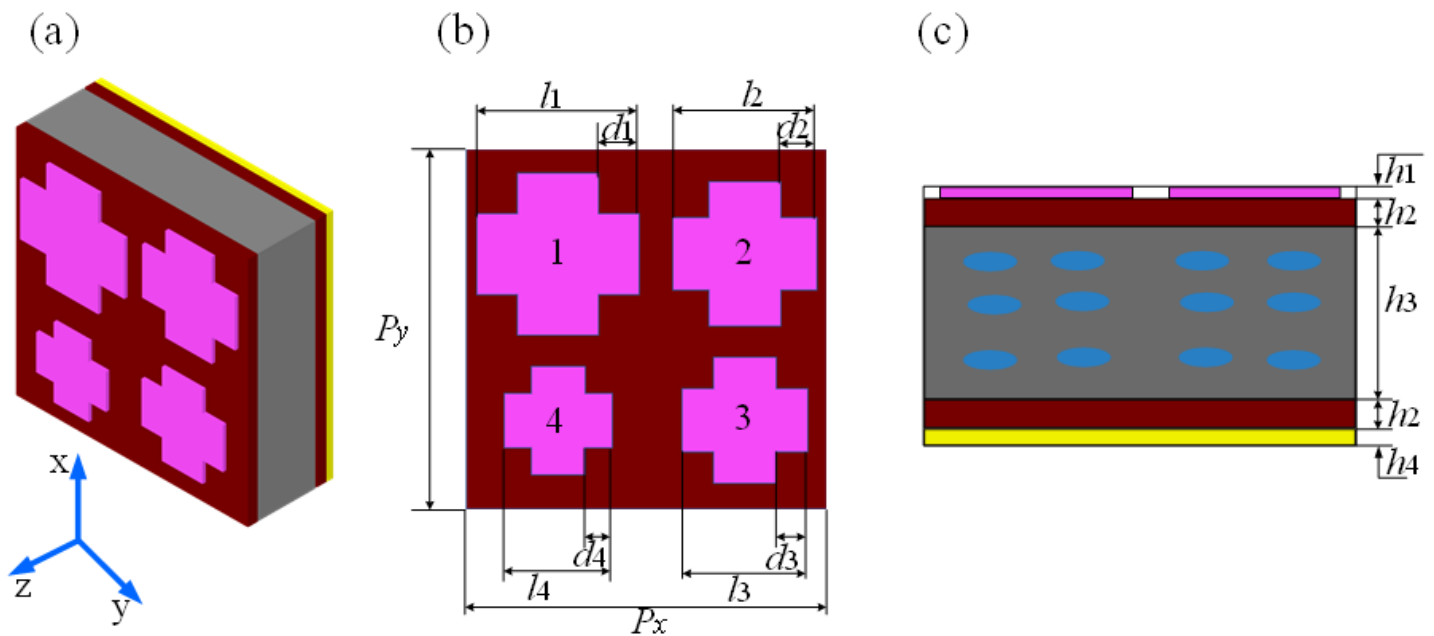


Figure 1

(a) 3-D THz broadband tunable absorber (b) Unit structure schematic of the absorber (c) The side view of the structure.

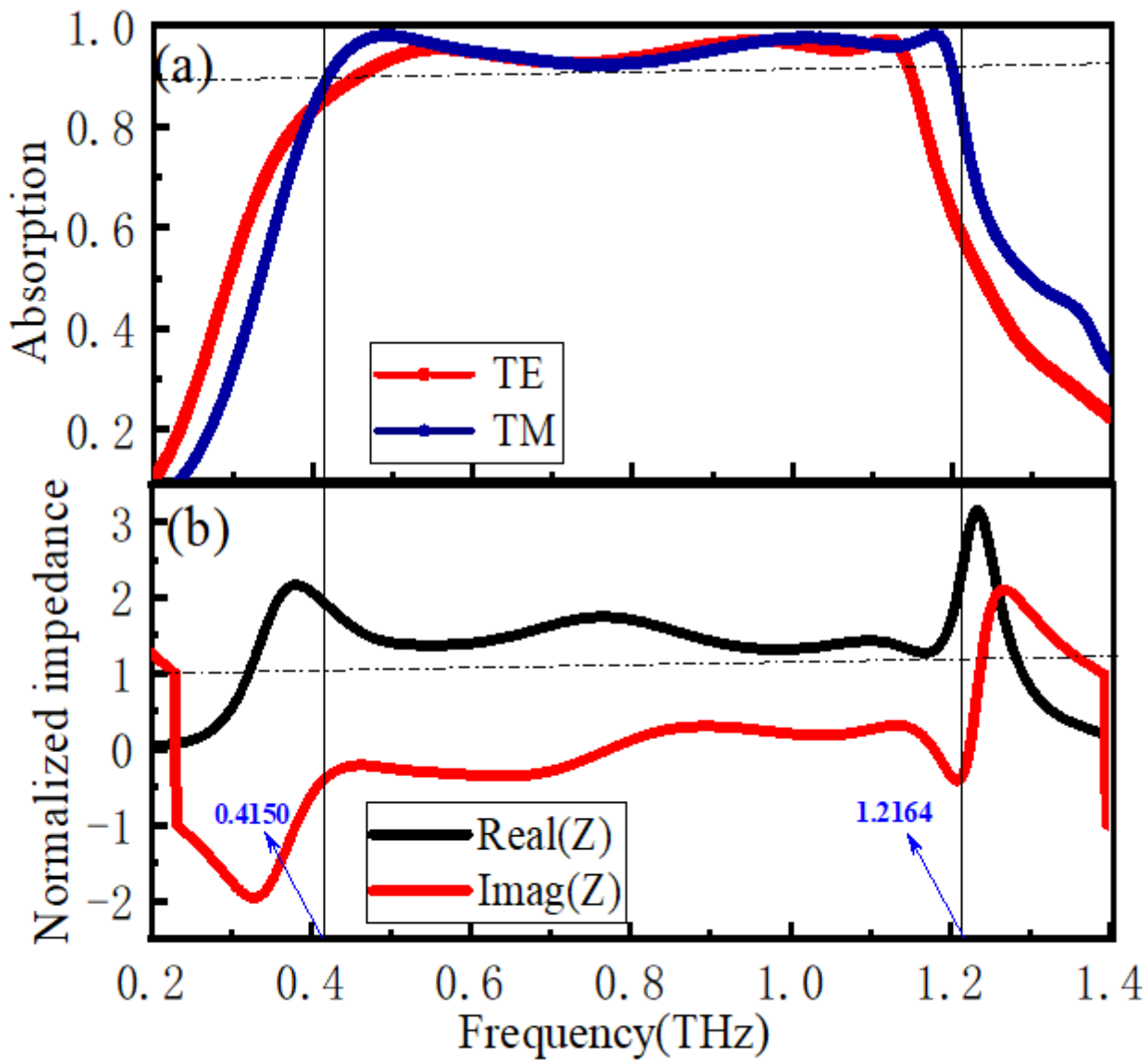


Figure 2

Absorption spectrum of terahertz broadband tunable absorber of (a) 0.9569 THz and 1.12 THz, (b) the matching impedance (Z) of the wideband absorber.

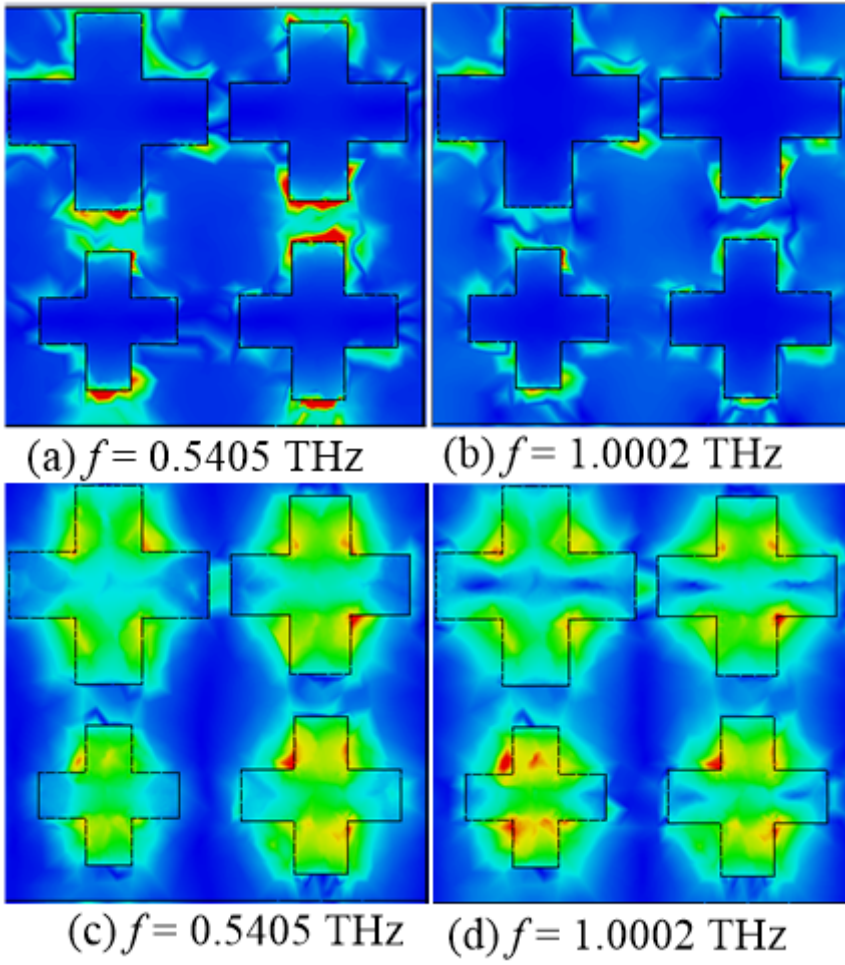


Figure 3

The distribution of electric at high absorption peaks of (a) $f = 0.5405$ THz , (b) $f = 1.0002$ THz and (c) and (d) show the distributions of corresponding magnetic field .

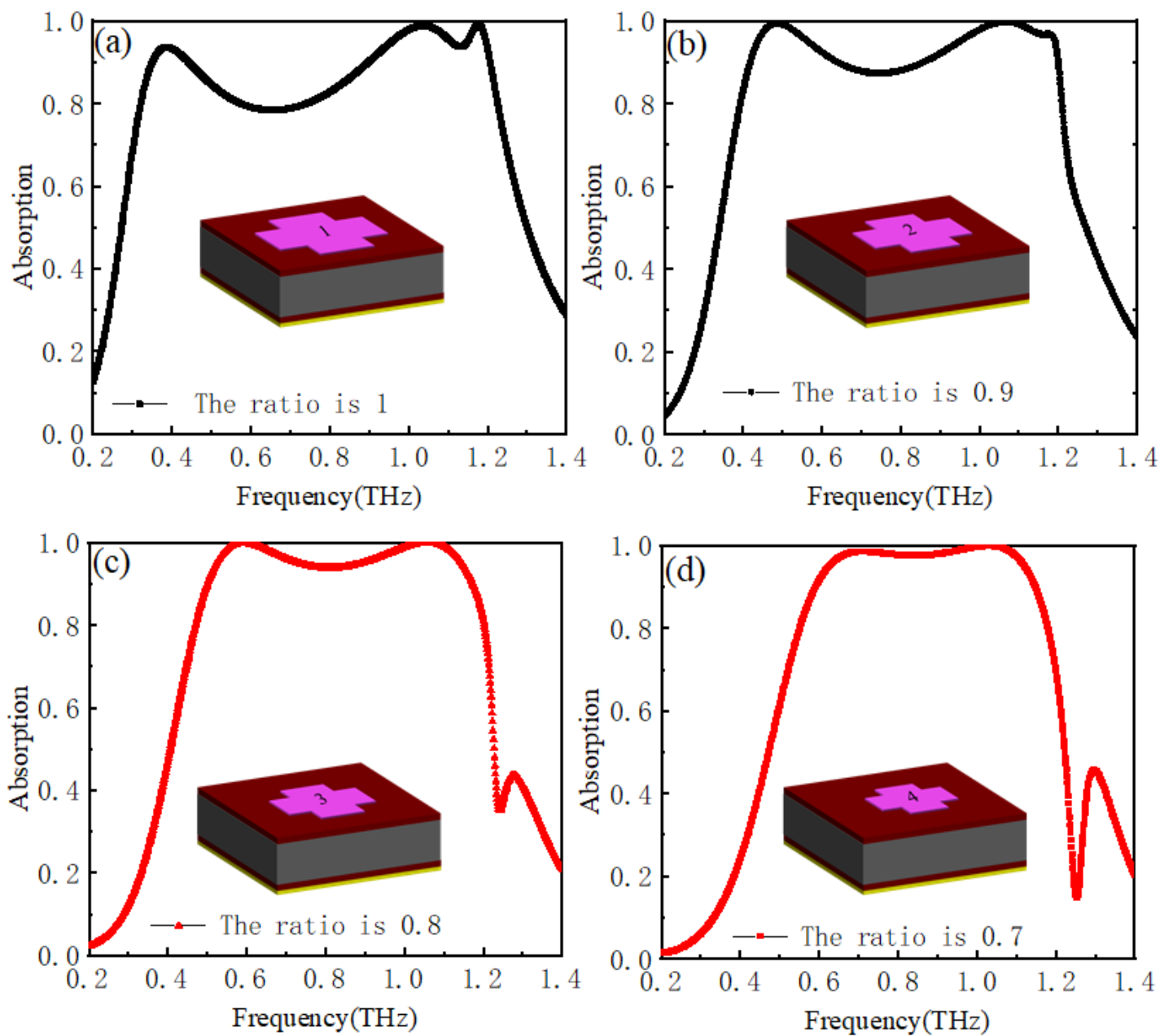


Figure 4

The absorption spectra are obtained and the corresponding geometrical structure is shown as follows: the ratio of single cross-shapes are 1,0.9,0.8, and 0.7, respectively.

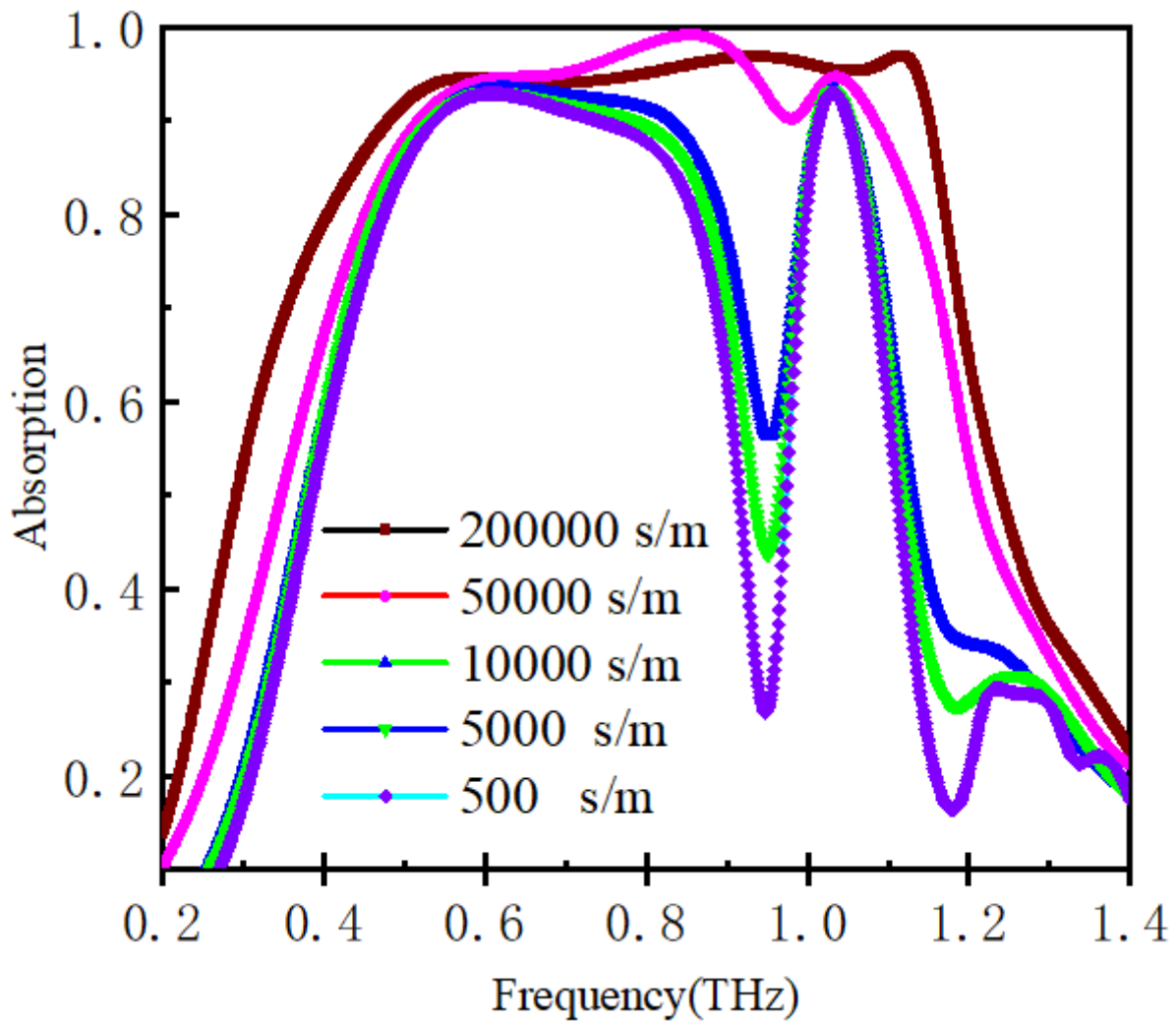


Figure 5

Resonant absorption of the broadband absorber in the lower terahertz region tuned by the conductivity of the VO2 film.

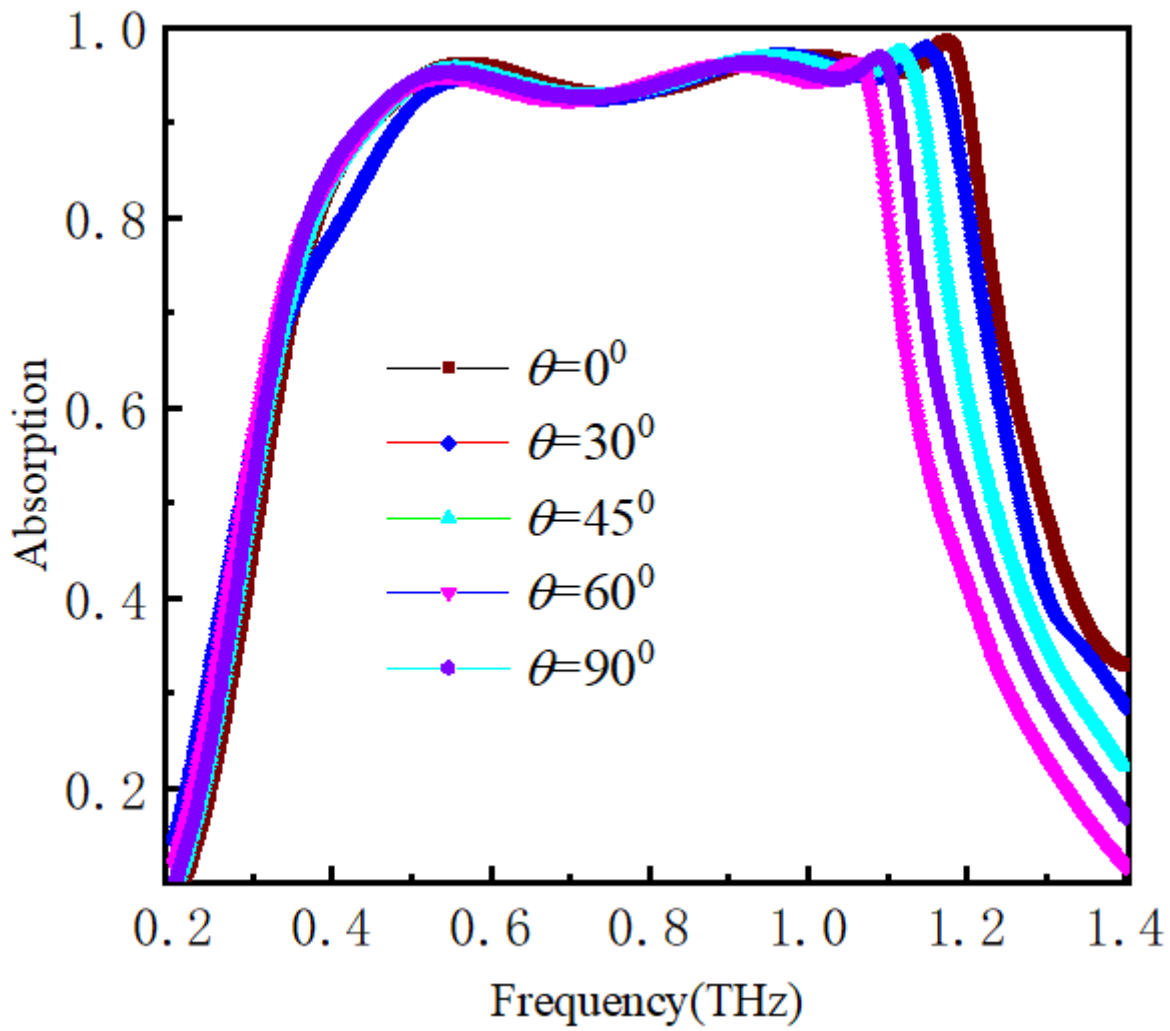


Figure 6

Under TM- polarized mode, the absorption THz spectrum of the absorber for different LC director angles θ as the bias voltage increases.

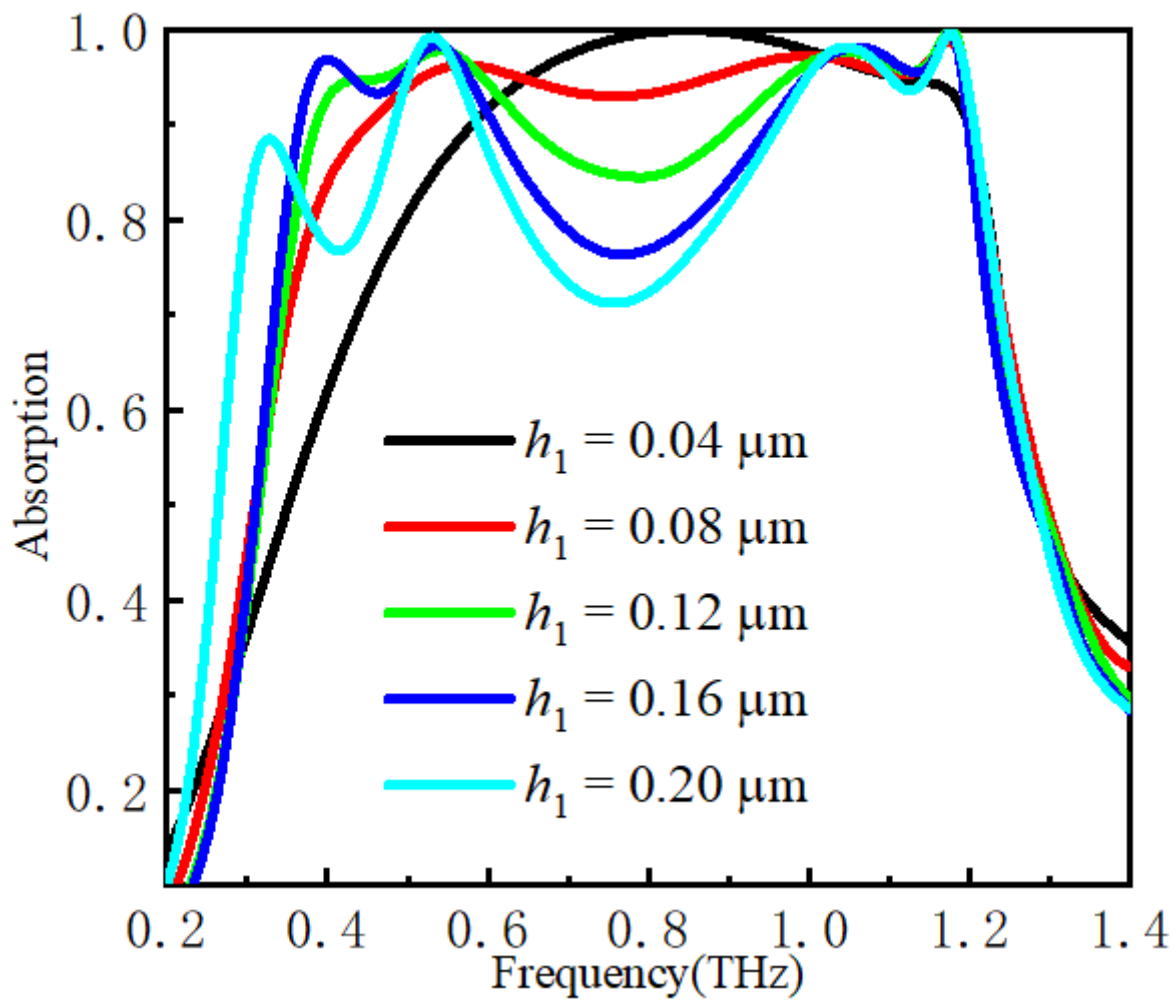


Figure 7

Absorption spectrum of the proposed absorber for different thickness of the VO₂ film from 0.04 μm to 0.20 μm .

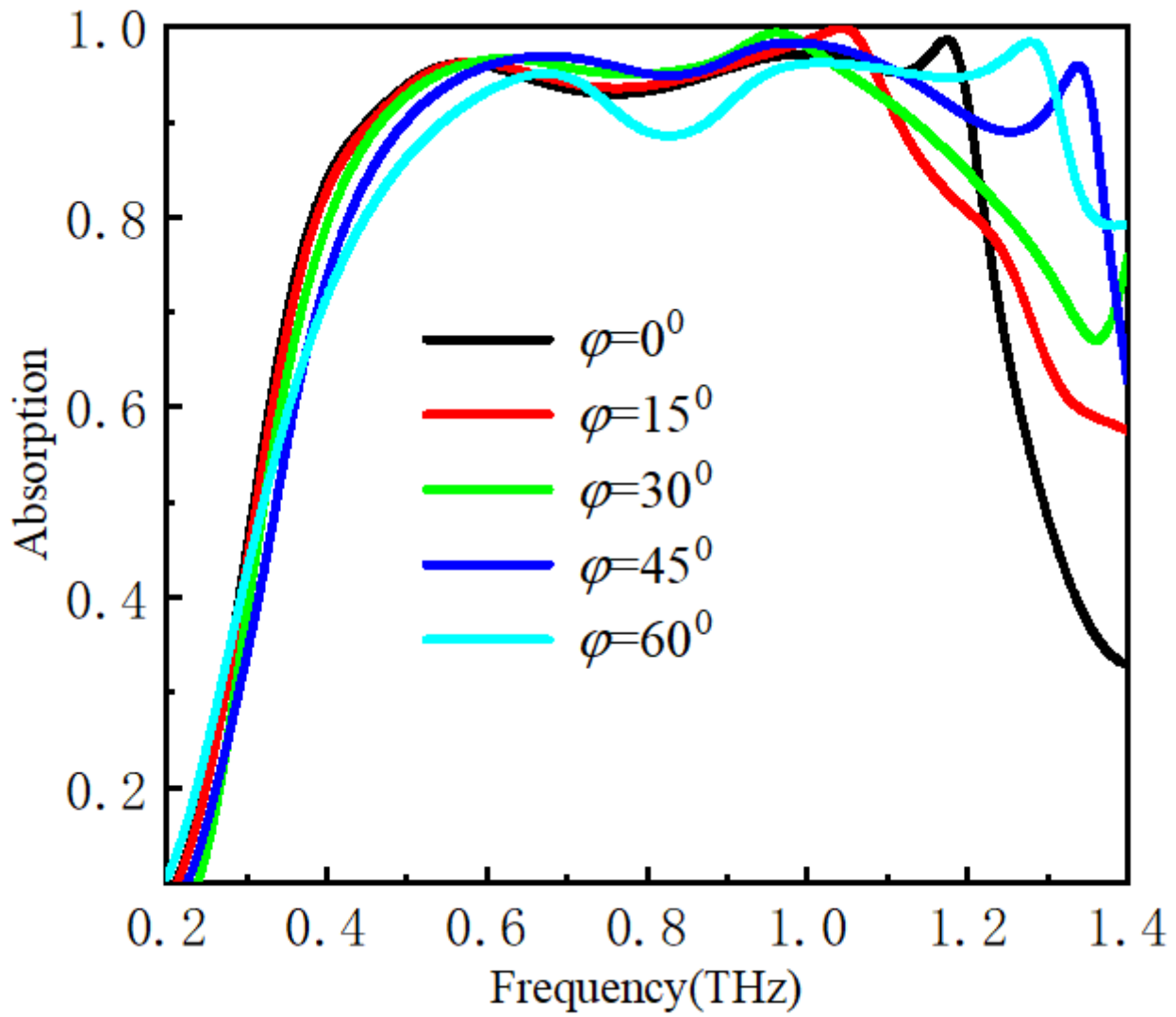


Figure 8

Absorption response of the absorber for different angles for TM polarization of incident wave φ from 0° to 60° .